Scientific Research Publishing

Fabrication, Microstructure, Thermal and Electrical Properties of Copper Heat Sink Composites

Walid Daoush[1,2], Ahmed Swidan[3], Gamal Abd El-Aziz[4], Mohamed Abdelhalim[4]

[1]Department of Production Technology, Faculty of Industrial Education, Helwan University, Cairo, Egypt
[2]Present Address: Department of Chemistry, Faculty of Science, Al-Imam Muhammad Ibn Saud Islamic University, Al Riyadh, KSA
[3]Mechanical Department, Ameeria Integrated Technical Cluster, Cairo, Egypt
[4]Mechanical Department, Faculty of Industrial Education, Suez University, Suez; Egypt
Email: waliddaoush@techedu.helwan.edu.eg

Abstract

Copper as well as copper base composites reinforced with coated and uncoated 1 wt% diamond, graphite particles or short carbon fibers are prepared by powder metallurgy process. The reinforcement particles were encapsulated with silver as well as copper layer by using the electroless deposition technique to investigate the influence of the reinforcement surface coating on the microstructure, density, electrical and thermal properties of the sintered samples. The coated and the uncoated powders were cold compacted at 600 MPa, and then sintered at 1173 K (900˚C) for 2 h under hydrogen atmosphere. The phase composition, morphology and microstructure of the prepared powders as well as the copper base sintered composites were investigated using X-ray diffraction analysis (XRD) and Scanning Electron Microscope (SEM) equipped with an Energy Dispersive Spectrometer (EDS) respectively. The density of the sintered composites was measured by Archimedes method. The copper base consolidated composites had a density up to 96% and the reinforcement coated particles were distributed uniformly within the copper matrix better than the uncoated one. The electrical resistivity at room temperature and the heat transfer conduction of the produced samples were measured in a temperature range between 323 K (50˚C) and 393 K (120˚C). The results observed that the sintered materials prepared from the coated powder have lower electrical resistivity than the sintered materials prepared from the mixed powders. On the other hand the thermal conductivity values were calculated using the heat transfer conduction values by means of the Fourier formula. The results observed that the thermal conductivity of copper is (391 W/m·K), 1 wt% diamond/Cu is (408 W/m·K), 1 wt% graphite coated silver/Cu is (393 W/m·K), 1 wt% Cu coated short carbon fiber/Cu is (393 W/m·K), graphite/Cu is (383 W/m·K) and short carbon fiber/Cu is (382 W/m·K). The obtained composites

are expected to be suitable for heat sink applications. The heat transfer testing experiments were done. The forced convection of the present work was done and compared with the previous work in the literature, and satisfactory agreement was achieved.

Keywords

Heat Sink, Powder Metallurgy Matrix Composites, Electrical Resistivity, Thermal Conductivity Natural, Forced Convection

1. Introduction

Cooling of electronic devices is very important to avoid temperature rising of its components during passing the current through it and slowing down its efficiency and destroying it. Cooling of electronic equipment using heat sink metallic materials is better than cooling by air due to the higher thermal conductivity of metals than air. Heat sink should be a passive component that cools a device by dissipating heat into surrounding air. Traditional heat sink and heat spreader is made of aluminum and copper with low Thermal Expansion Coefficient (TEC). New composite materials of suitable electrical and thermal conductivity for heat sink materials applications are required to prevent the failure of electronic equipment and high thermal stresses in electronic components resulting from temperature variations. The thermo-mechanical fractures may be formed during semiconductor chip production especially with temperature fluctuations from 323 K (50˚C) to 473 K (200˚C) and during cooling [1]. A design of a heat sink of Aluminum base for cooling of Printed Circuit Board (PCB) was used to dissipate about 19.5 watts of heat energy [2]. Al/SiC composite was used with acceptable properties. The graphite/metal composites represent a clear alternative to Al/SiC materials. The graphite-based composites are cheap and machinable, keeping at the same time very high thermal properties [3], [4]. Copper is indeed characterized by a high thermal conductivity but at the same time its high density (8.9 g/cm³) increases weight of the final product, which in most of the cases does not meet specific application requirements [5].

Powder metallurgy is one of the techniques used to fabricate sintered metallic heat sink materials from its powder. The sintered materials made from coated powders have better structure homogeneity and electrical resistivity than those made from mixed powders. Coated diamond particles have a uniform distribution in copper composite and the interface between diamond particles and *Cu* matrix [5]. Because diamond has TEC value of 2.3×10^{-6}/K higher 6 times than *Cu*. *Cu*/diamond composites with matched TEC are used to eliminate the high heat produced during semiconductor component operation. Also a mixture of graphite (*Gr*) and other materials may be used [7], [8].

It was founded from previous research work that the materials used in heat transfer such as aluminum/silicon carbide compared to copper are insufficient in cooling electronic devices [3], [4]. A new generation of heat sink materials was developed to en-

hance the thermal properties such as diamonds reinforced copper composites. However diamond in general is expensive and the consolidation of the materials needs high pressure and high temperature [6]. Researchers suggested using alternative materials such as graphite, short carbon fibers instead of diamond as reinforced materials [9], [10]. On the other hand some researchers improved the properties of the copper composites by powder coating with silver and copper before sintering [11], [12] and to increase the bonding between the copper matrix and the reinforcement particles by decreasing the air gap between the constituents.

The main aim of this research is to produce a material characterized by high thermal conductivity, low coefficient of thermal expansion, good mechanical properties, low density and good electrical conductivity. In this study copper matrix composites reinforced with diamond (*Di*) particles, graphite (*Gr*) particles, silver coated graphite particles, short carbon fiber (*CF*) and copper coated short carbon fiber are tested. The investigated reinforcement powders were mixed separately with copper powder and underwent cold compaction and sintering at 1123 K (850˚C) to prepare sintered copper matrix composites. The morphology of the powder as well as the microstructure of the sintered composites was investigated the test specimens were tested by optical, scanning electron microscopes and XRD. The physical, electrical and thermal properties were measured to evaluate the produced sintered composites.

2. Materials and Methods

2.1. Starting Materials

High purity electrolytic copper powder (99.9) with an average particle size of 44 μm was purchased from OXFORD laboratory reagent; India. *Gr*aphite and carbon short fiber were purchased from Austria institute of technology. Diamond, with particle size less than ~1 μm was provided from Iljin Co. LTD, South Korea. **Figure 1** shows SEM images with different magnifications of the starting copper powder, the diamond, graphite particles and the short carbon fibers. Silver nitrate, copper sulphate, potassium sodium tartarate, nitric acid, sodium hydroxide, formaldehyde and Ammonia solution were provided from El-Nasser Chemical Co. LTD. Egypt.

2.2. Methods

2.2.1. Fabrication of Copper Base Composite Powder

Graphite, diamond and short carbon fiber powders were treated by soaking and stirring in nitric acid for 5 min with stirring rat of 250 rpm. To clean and etching the surface of the particles. The treated particles and short fibers were cleaned by 50% sodium hydroxide solution to neutralize the excess of the nitric acid followed by acetone to dissolve any organic foreign matter. The obtained graphite particles underwent metallization and coating by electroless silver deposition in ammoniacal silver nitrate solution using formaldehyde as a reducing agent. On the other hand the treated carbon short fiber was metallized and coated by electroless copper deposition process using bath composition in **Table 1**. Five compositions were prepared by simple mixing in porcelain
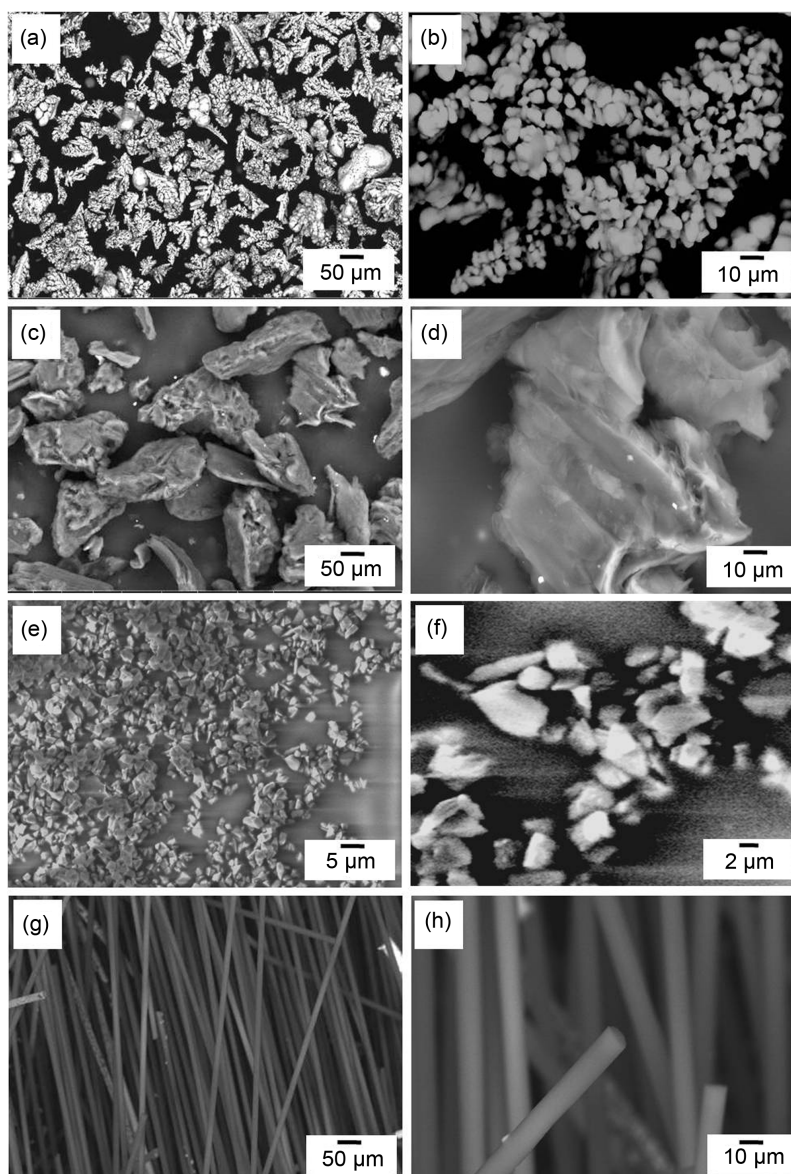
Figure 1. SEM images with different magnifications of the investigated powders. (a), (b) *Cu* powder, (c), (d) graphite, (e), (f) diamond powder and (g), (h) carbon short fiber.

Table 1. The chemical composition of the electroless nickel baths which used to prepare sample coated with copper powder.

Chemical Composition	Condition
Copper sulphate	35 g/l
Potassium sodium tartrate	170 g/l
Sodium hydroxide	50 g/l
Formaldehyde	200 ml/l
pH	~12
Temperature	25°C

mortar with 1 wt% paraffin wax of diamond, graphite, short carbon fiber, graphite coated silver and carbon fiber copper coated with copper powder. A reference copper sample was prepared under same conditions [13].

2.2.2. Consolidation of Copper Base Composite Powder

The obtained mixtures as well as the pure copper powder samples underwent cold compaction at 600 MPa in a uniaxial die of dimension (50 mm diameter and 150 mm length). The green compacts were sintered under mixture of hydrogen/nitrogen gas at 1173 K (900°C) for 2 h (see the sintering cycle in **Figure 2** [14]).

2.2.3. Microstructure and Density Measurements

The produces powders as well as the sintered compacts underwent microstructure investigations and chemical analysis by using SEM model QUANTA FE250-EDAX Genesis and XRD model Bruker advanced X-ray diffract meter model D8 Kristalloflex.

The properties of the sintered samples were evaluated by measuring the density according to MPIF Standards 42, 1998, using Archimedes rule. The density (ρ) of the samples was calculated according to Equation (1) [15], [16].

$$\rho = W_a / (W_a - W_w) \rho_{\text{water}} \text{ gm}/\text{cm}^3 \tag{1}$$

where the of densities Cu (8.94 g/cm³), Gr (2.17 g/cm³), C_F (2.15 g/cm³), Di (3.48 - 52 g/cm³), and W_a and W_w are the weights of the samples in air and water respectively [12], [13].

2.2.4. Thermal Properties of Copper Base Composites

The thermal conductivity of the prepared sintered samples was measured by the conduction method. The thermal heating test was done by an electrical heater. It consists of an electrical isolated plate heater 1000 W, 220 V, 50 Hz. It was insulated with one inch insulator at all directions. One hole from the top of the heater is drilled to force the heat transfer in only one direction. Two groves were made at the outside surface and two thermocouples are put inside groves to measure the temperature of heater surface.

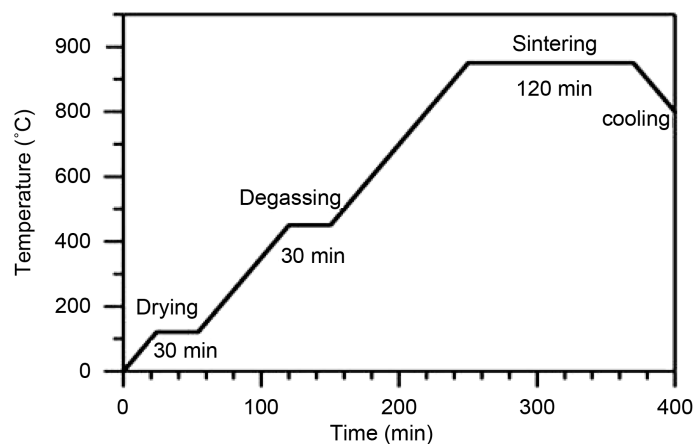The heat transfer conduction is determined by measuring the temperature difference

Figure 2. Heating cycle for sintering process in hydrogen atmosphere.

between the upper and the lower surface of the prepared samples as a function of time by means of five K type thermocouples distributed on the specimen surface and was fixed above one inch isolated hot plate. The thermocouples were connected with a multipoint swatch. The output from the multipoint swatch was connected with digital thermometer type K to record the temperature. The volt and current pass through the specimen were measured by electric meter. Figure 3 shows the experimental setup circuit of measuring the temperature gradient under controlled temperature range from 293 K (20˚C) to 473 K (200˚C).

The thermal conductivity was calculated by substituting the values of current, volt, temperature, area and thickness of the samples in the Fourier formula [4] as the average temperature and calculated from the Equation (2).

$$q = -KA\left(\Delta t/\Delta x\right) \tag{2}$$

where (A), the cross section area in (m^2), (K) the thermal conductivity in W/m·K, (q), the power (W), (Δt) temperature difference in (K), and (Δx) thickness for heat sink, (m). The experimental test rig is designed to measure the thermal conductivity.

The heat transfer convection was calculated by natural convection and forced convection from the Equation (3) [17]-[32].

$$q = h_c A\Delta T \tag{3}$$

where h_c = convective heat transfer coefficient of the process W/(m^2·K). The average Nusselt number for horizontal surfaces can be determined from the simple power-law relations. The hydraulic characteristic length for horizontal surfaces is calculated.

In natural convection:

The dimensionless parameter represents the natural convection effects, and is called the Grashof number Gr_L. [17]-[32].

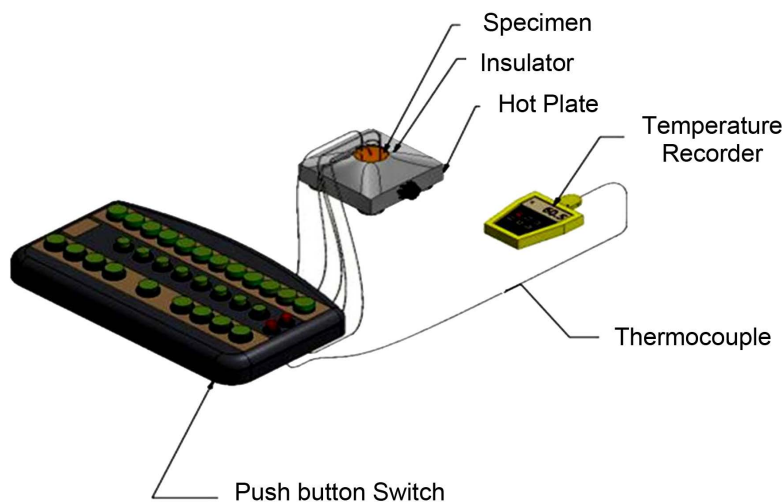$$Gr_L = \frac{g\beta\left(T_s - T_\infty\right)L^3}{v^2} \tag{4}$$

Figure 3. The experimental setup circuit of measuring the thermal conductivity.

where *Ra* is the Rayleigh number, which is the product of the Grashof and Prandtl numbers [17]-[32]:

$$Ra = Gr \times Pr \tag{5}$$

In forced convection, the experimental data for heat transfer is often represented conveniently with reasonable accuracy by a simple power-law relation of the form [17]-[32].

$$Nu = C \times Re_L^m \times Pr^n$$

$$Nu = \frac{hl}{k}, \quad Nu = 0.27 Ra_{Lc}^{0.25} \tag{6}$$

where
g = gravitational acceleration, m/s^2
β = coefficient of volume expansion, 1/K (*β* = 1/*T* for ideal gases)
T_s = temperature of the surface, ˚C
T_∞ = temperature of the fluid sufficiently far from the surface, ˚C
L_c = characteristic length of the geometry, m
v = kinematic viscosity of the fluid, m^2/s.
m and *n* are constant exponents and the value of the constant (*C*) depends on geometry and flow.

$$Nu = \frac{hl}{k} = 0.683 Re^{0.466} L_D Pr^{0.3} \tag{7}$$

where *Re* ranged 40 : 4000.

2.2.5. Electrical Properties of Copper Base Composites

The electrical resistivity of the sintered materials was measured using the four probe method by using Omega *CL* 8400 micrometer device. The rectangular sintered specimen was placed in a specially designed for making the electrical connection. The resistivity (R_o) was calculated according to Equation (8)

$$R_o = (R \cdot A)/L \tag{8}$$

where R_o the resistance in μΩ·m and *R* the resistance in μΩ.

3. Results and Discussion

3.1. Powder Fabrication and Characterization

A pretreatment process was employed to remove organic and nonorganic impurities and improve the surface properties of the reinforcement particles (diamond, graphite particles and short carbon fiber) by using fairly aggressive chemicals. Sodium hydroxide (50% conc.) and nitric acid (67% conc.) was used to dissolve any inorganic impurities such as metals but acetone was used to remove the other organic impurities, such as greases or oils. The pretreated reinforcement was activated by silver deposition method. The silver deposition system takes place using a solution of silver nitrate and ammonium hydroxide to form silver layer on the graphite particles using formaldehyde as a

reducing agent. **Figure 4(a)** and **Figure 4(b)** shows SEM images with different magnifications of the coated graphite particles with silver. It was observed that the graphite particles is completely coated and encapsulated by silver metal layer. On the other hand the pretreated short carbon fibers were encapsulated by copper layer using the autocatalytic electroless deposition of copper metal on its surface shows the morphology of the coated short carbon fibers with copper and its composition (see **Figure 4(c)** and **Figure 4(d)**). The copper is uniformly deposited on the short carbon fiber. **Figure 4(e)** shows an EDAX analysis of the copper coated short carbon fibers and provides a complete chemical composition of the coated short fibers which is composed of copper and carbon.

Figure 5(a) and **Figure 5(b)** shows the X-ray diffraction patterns of the investigated powders and the corresponding sintered composites to assess the formation of phase's transformation. It was observed from the results that the X-ray diffraction patterns of
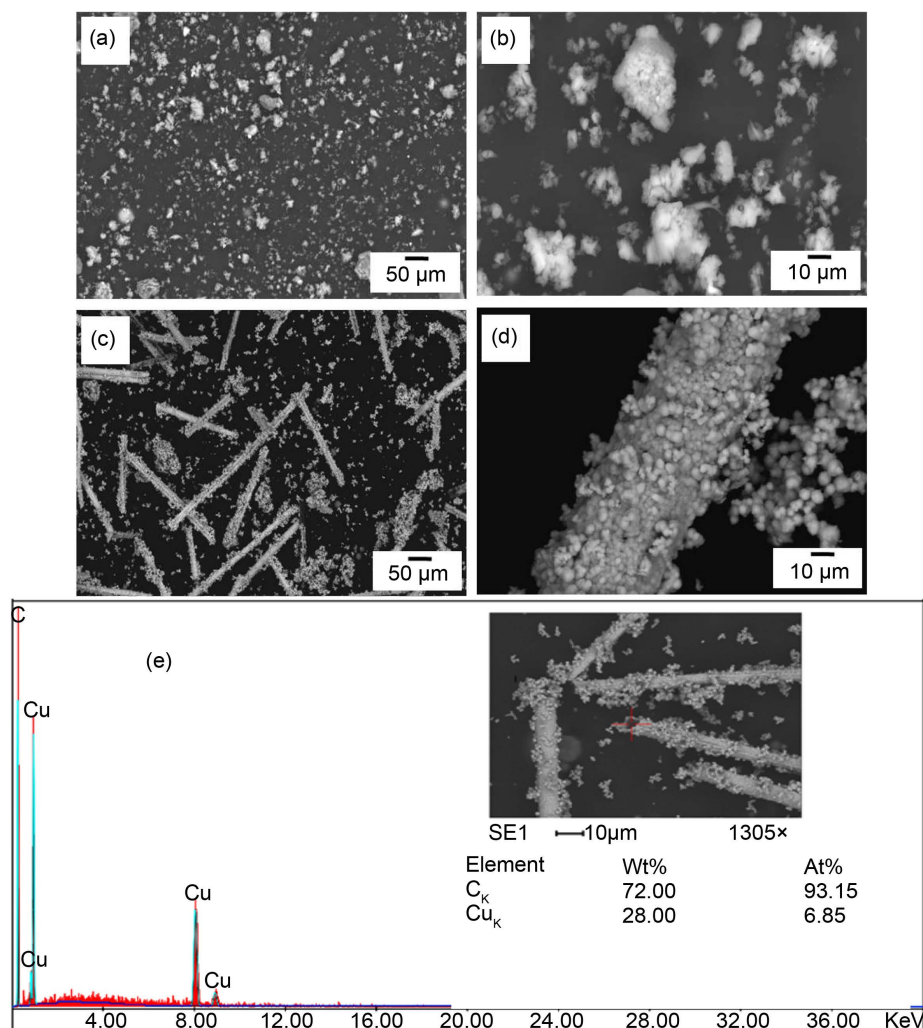

Element	Wt%	At%
C_K	72.00	93.15
Cu_K	28.00	6.85

Figure 4. SEM images with different magnifications and EDAX analysis of the prepared coated powders; where (a), (b) silver coated graphite particles, (c), (d) copper coated carbon short fiber and (e) the EDAX compositional analysis of the copper coated carbon short fiber.
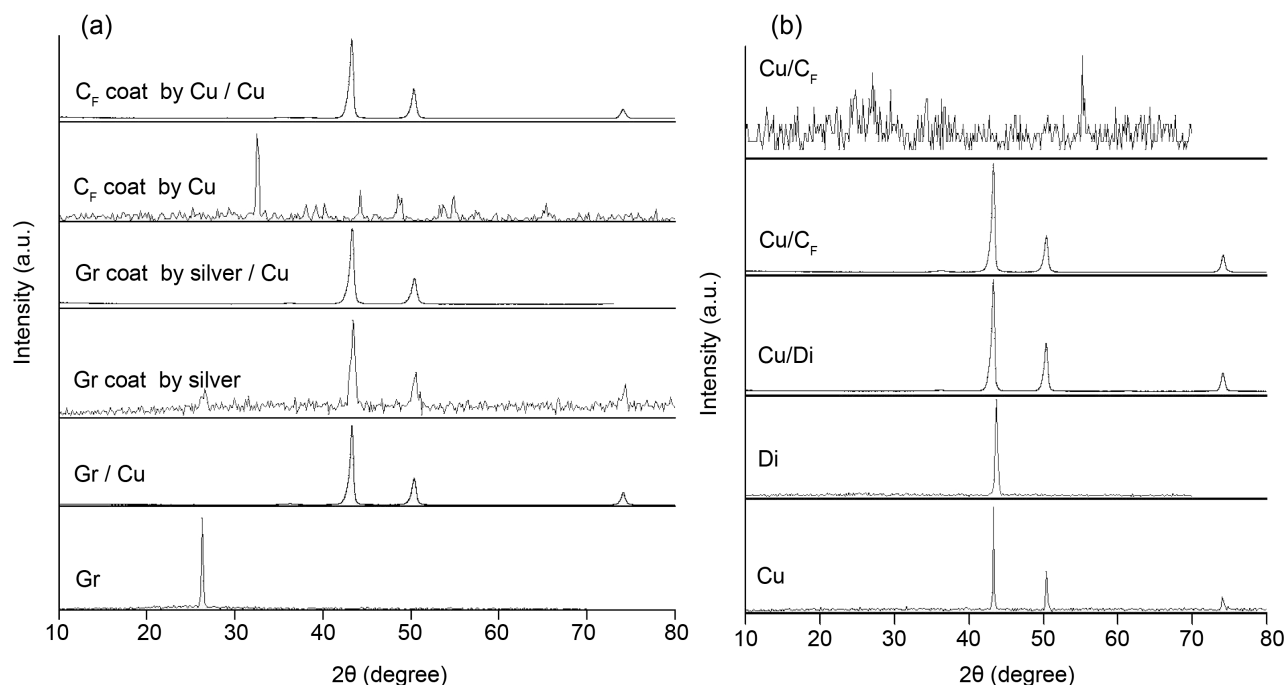
Figure 5. X-ray diffraction patterns of the investigated powder, the coated powders and the copper base sintered composites.

the powder as well as the sintered copper matrix composites shows peaks of only copper metal and the reinforcement particles and there are not any foreign peaks of any contaminates or new phase. It is due to the non interaction between the copper metal and the reinforcements during the sintering process. The crystal size of *Cu* and different reinforcements materials were calculated from the X-ray line broadening using Scherer's formula ($D = 0.9\lambda/B\cos\theta$) [16], where; *D* is the crystallite size, λ is the wavelength of the radiation, θ is the Bragg's angle and B is the full width at half maximum. The average size of *Cu* (88 nm), *Gr* (60 nm), *Gr* coated silver (56.4 nm), *Di* (57.1 nm), C_F (8.1 nm) and C_F coated *Cu* (25.3 nm). Showed that all of the fee equal values because cu ratio equal to 99 wt% of all values and other materials 1 wt% in all other.

Consolidation of the metallic powders is mainly carried out using compaction followed by sintering. Sintering is a thermal process which increases the strength of a powder mass by bonding adjacent particles via diffusion or related atomic level events. As a result of this process, the material acquires the required physical and mechanical properties. Most of the properties of a powder compact are improved with sintering [15].

The microstructure of the prepared copper matrix composites were investigated by SEM after grinding and polishing of the sample cross section. **Figure 6** shows Back Scattered Electron (BSE) images for the produced copper base composites containing different reinforcements of *Di*, *Gr*, *Gr* coated silver, C_F, C_F coated *Cu*. During scanning using the backscattered electron detector, the higher the average atomic number of the area being analyzed, the greater the probability is that a (BSE) will be generated. As a result, BSE images display atomic number contrast with brighter regions being generated from areas of higher average atomic number. In other words, the BSD images easily
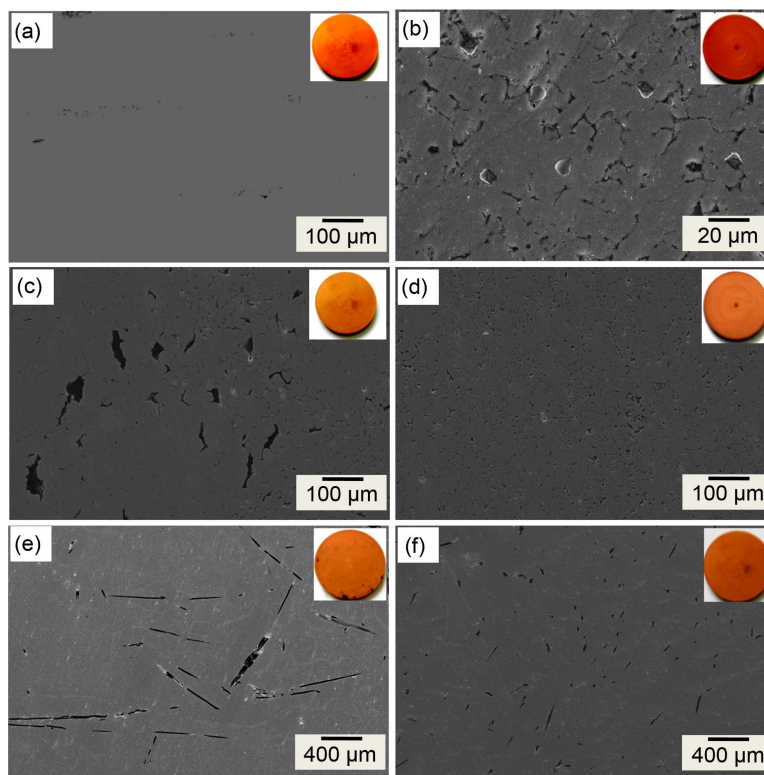
Figure 6. SEM micrographs of the produced copper base sintered composites; where (a) Cu pure, (b) *Cu*/*Gr* one wt%, (c) *Gr* coated silver one wt%, (d) *Cu*/one wt% *Di*, (e) *Cu*/one wt% C_F, (f) *Cu*/one wt% C_F coated *Cu*.

show the difference between the different phases (areas of different atomic number) through the difference in contrast. The result observed that the reinforced materials (diamond, graphite or carbon fiber) were homogeneously distributed in the copper matrix. In addition the coated reinforcement materials (graphite coated by silver and carbon fiber coated by copper) were strongly bonded by the copper matrix due to the improvement in the wet ability between the coated reinforcement particles and the copper matrix. Also the porosity of the treated reinforcements by coating has lower values than the composites prepared by mixing of its constituents. Since the uncoated reinforcements are easy to be stripped off during mechanical polishing, small pits are left on the surface of samples. While, the composite made from the coated reinforcements have lower porosity content due to the good contact between the particles and the matrix during sintering, and the metallic binders decrease all the existing cavities between *Cu* particles.

Figure 6(a) and Figure 6(b) shows SEM micrographs for the sintered pure *Cu* and the corresponding 1 wt% diamond particles/*Cu* coated composites. The microstructures show good sinterability and a homogeneous distribution of the diamond particles in the copper matrix. Figure 6(c) and Figure 6(d) illustrates SEM micrographs for the sintered 1 wt% uncoated graphite/*Cu* and 1 wt% graphite/*Cu* silver coated composites. On the other hand Figure 6(e) and Figure 6(f) illustrates SEM micrographs for the

sintered 1 wt% uncoated short carbon fiber/*Cu* and 1 wt% short carbon fiber/*Cu* coated composites. The micrographs show that, the sintered materials prepared by electroless coating method have higher bonding between the graphite particles as well as the short carbon fibers and the *Cu* matrix with low-porosity contents. The reason behind increasing the bonding and density of *Cu*-coated composites is mainly due to the good sinterability as a result of the encapsulation of short carbon fibres with *Cu*, the particle/particle contacts are mainly *Cu*/*Cu* contacts and sintering behaves like *Cu* compacts sintering. In order to determine the distribution of the elements in the sample a compositional analysis was performed by EDAX. **Figure 7(a)** and **Figure 7(b)** shows
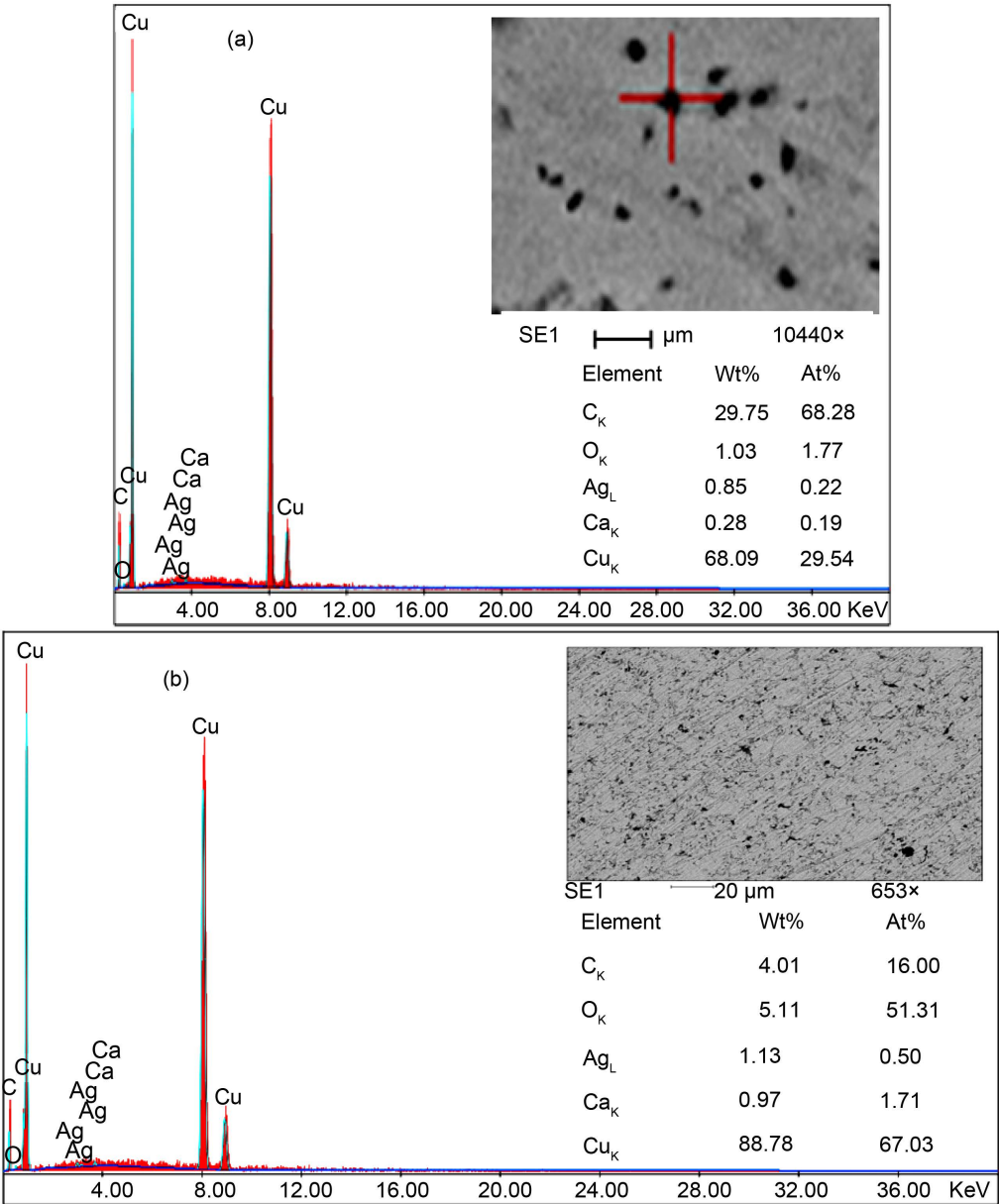

Figure 7. SEM images with EDAX compositional analysis of the produced copper base sintered composites; where (a) 1 wt% Diamond/*Cu*, (b) 1 wt% Graphite/Cu.

reprehensive images and EDAX compositional analysis of 1 wt% *Gr*aphite/*Cu* and 1 wt% Diamond/*Cu* sintered composites. The reinforcement particles were appeared to have a dark color and this was being confirmed by the EDAX analysis.

3.2. Density of Sintered Copper Base Composites

The density of the powder metallurgy products is one of the most important properties which reflect the sinterability and the effect on the other properties. It is very sensitive to composition and porosity in the sample.

Figure 8 shows the density values of the green compacts as well as the sintered density and its relation with the porosity of the produced copper base composites. It was observed from the results that the relative green densities as well as the relative sintered density of the coated particles have higher values than the uncoated one. It was due to the good distribution and homogeneity of the coated particles inside the copper matrix which decrease the reinforcement's particle-particle interaction and decrease the grain growth. In addition the low-porosity contents of the coated particles due to the strong adhesion between the *Cu* matrix and reinforced particles. The reason behind decreasing the porosity and increasing in the density is the encapsulation of the reinforced particles with *Cu* and the particle-particle contact are mainly *Cu-Cu* which improve the adhesion between the particle and the copper matrix and improving the consolidation of the compacts during the sintering process.

3.3. Thermal Conductivity

Table 2 listed the obtained thermal conductivity values of the produced copper base sintered materials. As seen, the thermal conductivity of the uncoated *Cu* composites is significantly lower than the thermal conductivities of the coated composites. However the thermal conductivity of the pure copper metal is higher than the composites. This feature indicates low interfacial bonding of the uncoated reinforcement particles (diamond, graphite and short carbon fiber), owing to the non-wetting of *Cu* and the reinforcement particles. With particle coating process the interfacial bonding gets better. It can be concluded that the interfacial thermal conductance of coated type *Cu* base
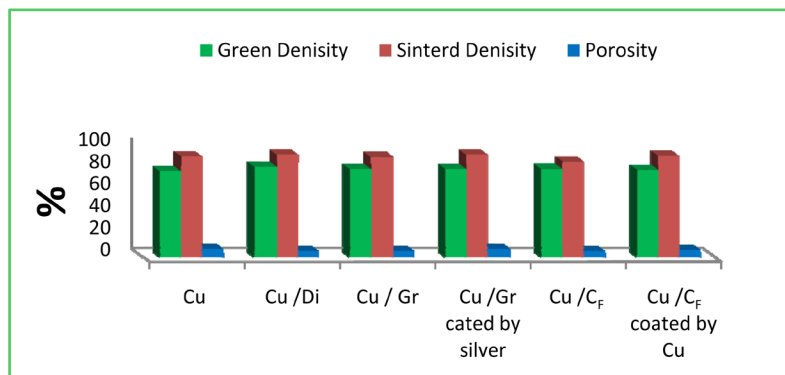

Figure 8. The relative green density, relative sintering density and porosity values of the produced copper base sintered composites.

Table 2. The thermal conductivity value of the produced copper base sintered composites.

Sample Composition	Thermal Conductivity, W/m·K
Copper	398
Cu/Diamond	405
Cu/ *Gr*	391
Cu/ *Gr* coated by silver	393
Cu/Carbon fiber	390
Cu/carbon fiber coated by copper	393

composites is much higher than that of uncoated one. It is due to the interface in the uncoated *Cu* base composites is filled in with a layer of air because *Cu* is non-wetted to diamond, graphite and short carbon fiber (see **Figure 6**). The low thermal conductivity of air, 0.026 W/m·K, offsets the high thermal conductivity of the reinforcement particles. The formed silver as well as *Cu* coated particles reduces the air gap improves the thermal conductivity of the coated composites. However, most of the interface is still filled in with air due to the small amount of the deposited silver as well as the copper metal. Most of the graphite and short carbon fiber surface were encapsulated with silver or copper, even though there are still few air gaps at the interface. As a result of too much amount of deposited silver or copper encapsulate the reinforcement particles, an undesirable thick *Ag* or *Cu* layers are coate the graphite particles or short carbon fibers surface, as seen in **Figure 4**. Certainly, the *Ag* or *Cu* layer could be tailored to a thinner one to reduce the undesirable interfacial thermal resistance. This can be regarded as an optimized interface in this study [16], [33]-[42].

Table 2 also shows the variation of the thermal conductivity of the produced sintered copper and its composites at temperature rang 323 - 393 K (50˚C - 120˚C). The thermal conductivity of 398 W/m·K was obtained for sintered *Cu*. This result is reasonably consistent with the thermal conductivity value of sintered *Cu* reported by Davis [38] as well as by Kim *et al.* [40].

It is clear from **Table 2** that the thermal conductivity increased in case of *Cu*/diamond composite to be 405 W/m·K. **Figure 9(a)** and **Figure 9(b)** shows the influence of temperature on the thermal conductivity of the prepared samples. It is observed that as the temperature increases; the thermal conductivity decreases in case of pure copper as well as *Cu*/diamond composite. It is also observed that the thermal conductivity of *Cu*/Diamond is higher than the thermal conductivity of pure copper by 3.5%. From the above results it can observed that the diamond improved the thermal conductivity of the *Cu*/diamond composite. The additions of diamond particles to *Cu* matrix increase the thermal conductivity of pure *Cu*. The low thermal conductivity of this composite was indicating a high thermal barrier resistance. This result due to separation between copper and diamond particles are which lead to low chemical affinity between copper and surrounded by cavities, diamond. Therefore, it is difficult to produce a bond of low thermal resistance and high mechanical strength between the matrix and the reinforcement.
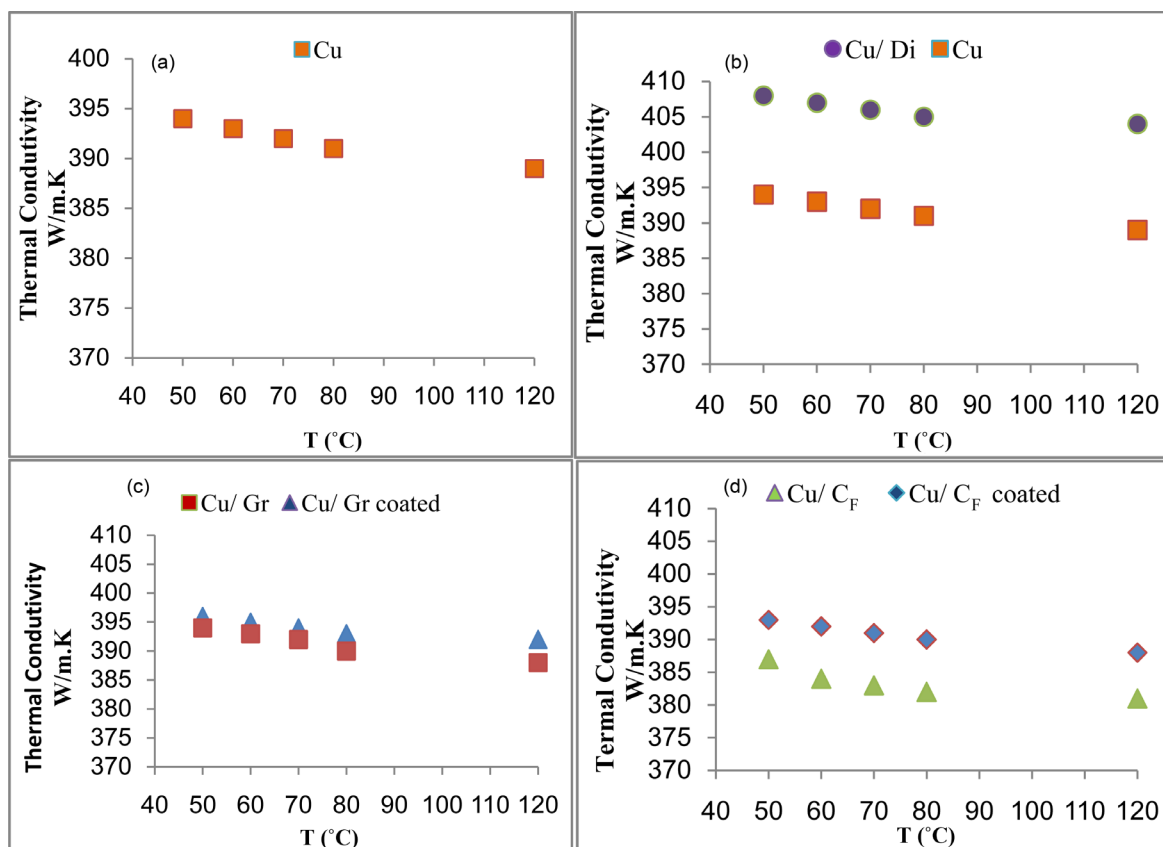
Figure 9. The influence of temperature on thermal conductivity of (a) copper, (b) copper and *Cu*/Diamond, (c) *Cu*/Graphite and (d) *Cu*/Carbon fiber at a temperature range 232 - 393 K (50˚C - 120˚C).

In case of graphite silver coated, the thermal conductivity has the mean value of 394 W/m·K as shown in **Figure 9(c)**. The results also show that the densification of the materials has a significant influence in the thermal conductivity. This reduction could also be due to the orientation of the measured thermal transport which could be different to the orientation of carbon fiber in the *Cu* matrix after consolidation. The random distribution of carbon fiber orientation could disturb the unidirectional heat transfer which could result in the reduction of the effective heat conduction of carbon fibers [41]. It is clear that a considerable increase of thermal conductivity is observed due to the coating of the graphite particles with copper improve the bonding between the graphite particles and the copper matrix which decrease the voids located in the interface between the graphite particles and the copper matrix and enhance the electron transfer through the sintered material. This increase is about 0.5% at 323 K (50˚C) and 1% at 393 K (120˚C). This means that the effect of silver coating of *Cu*/graphite is increase the total thermal conductivity by increasing the temperature. In case of carbon fiber coated by *Cu* the mean thermal conductivity is 393 W/m·K as shown in **Figure 9(d)**. It was observed that the coating process of *Cu*/carbon fiber by *Cu* increases the thermal conductivity by about 1.25% at 232 K (50˚C) and by 1.75% at 393 K (120˚C). While the reinforced particles lead to increase the thermal conductivity of the compo-

sites and coated material, which demonstrated the effectiveness of the coated layer to obtain a good thermal contact between the matrix and powder particles [4].

3.4. Electrical Resistivity and Conductivity

The electrical resistivity values of the fabricated composites are shown in Figure 10. It can be noticed that the electrical resistivity for investigated coated composites is lower than the uncoated one. It is evident that the electrical conductivities of the composites depend on the electrical conductivity of each component, volume fraction of the reinforcement, distribution and size of the reinforcement, density, and bonding between matrix and reinforcement as well as the synthesis method. It is known that the adhesion between diamond, graphite and carbon fiber and *Cu* matrix is very weak, because some nanosized interfacial gaps are often observed (see Figure 7). According to the *C*/*Cu* phase diagram, the *C* solubility in *Cu* is negligible. In addition, copper is known to be chemically inert with respect to carbon. The chemical incompatibility of carbon and copper can result in a weak mechanical interfacial bonding between diamond and graphite particles as well as short fiber and *Cu* matrix, therefore to severely reduce the electrical conductivity of the uncoated composite. An improved interfacial adhesion, by contrast, was obtained due to the formation of a continuous silver or copper interlayer of metalized graphite or carbon fibers, and in turn facilitated the enhancement of the composite electrical conductivity. Under the premise of ensuring the ability to form a good combination between diamond and graphite particles as well as short fiber with the *Cu* matrix [42].

3.5. Heat Transfer Convection Test

There are six specimens with deferent materials this (*Cu*, *Cu*/Diamond. *Cu*/*Gr*, *Cu*/*Gr* coated silver, *Cu*/*C_F*, *Cu*/*C_F* coated *Cu*). The convection test was done in to cases of natural, forced convection.

Figure 11 shows the results relation between (*Ra*) and (*Nu*) of the specimen. It is
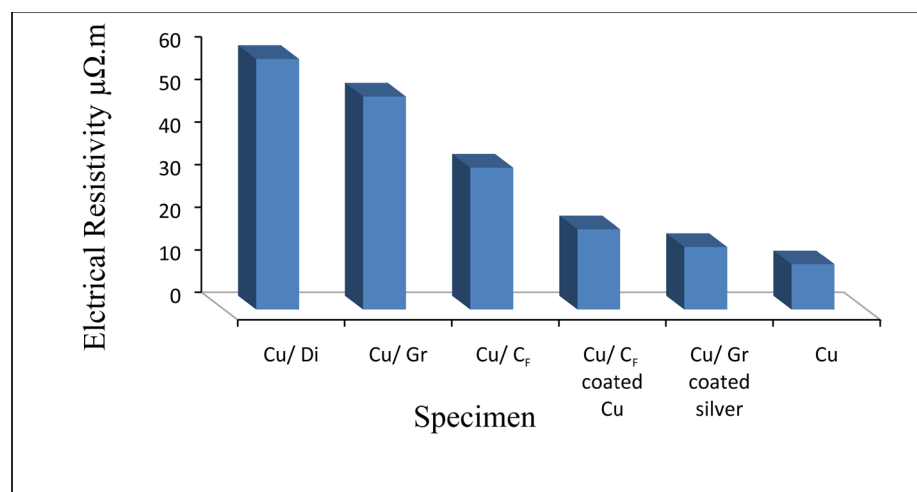

Figure 10. The electrical resistivity values of the produced copper base sintered composites.
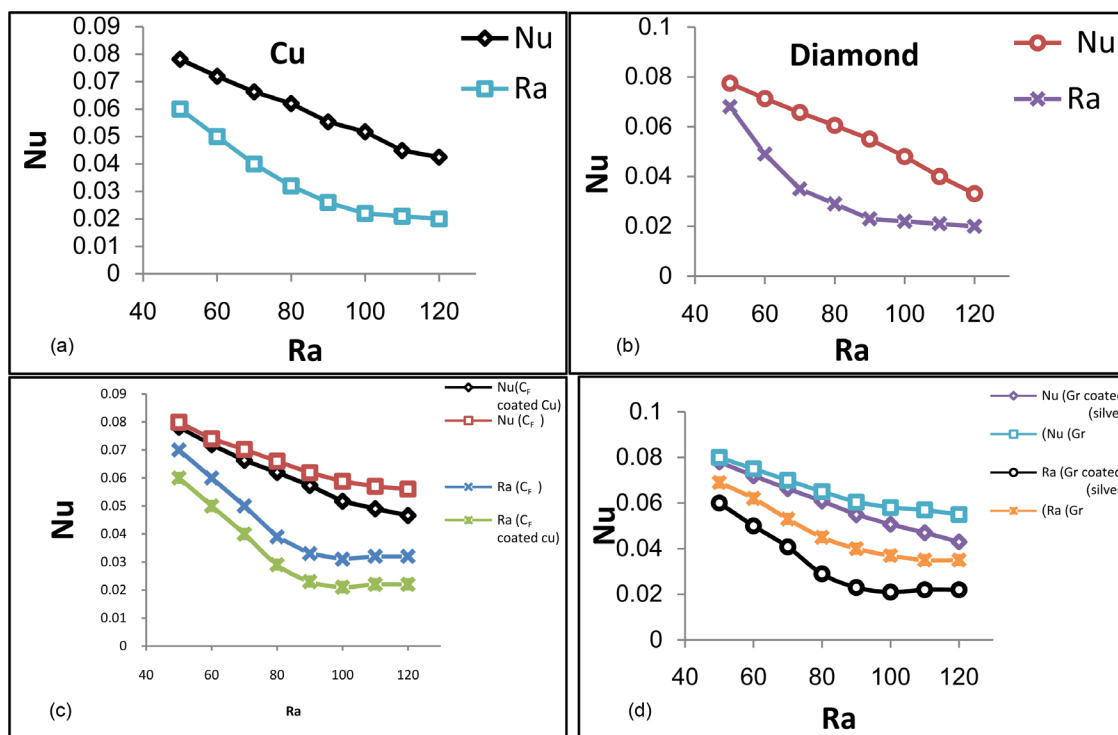
Figure 11. (*Ra*) versus (*Nu*) cases of natural convection for the prepared sintered samples.

clear that the values of *Nu* are decrease with increase of *Ra* due to the increase of the air temperature which is the density of a decrease the phenomena lead to decreasing the *Ra* number.

In forced convection **Figure 12** explains the relation between the Reynolds and Nusselt number in cases of the forced convection tested. It is clear that the values of *Re* constant with difference spacemen because the constant velocity. The value *Re* number ranged 40 - 4000. The *Nu* are difference with other spacemen The relation between local Nusselt number and local (*Re*) number which obtained from experimental results.

$$Nu = \frac{hl}{k} = 0.683 Re^{0.466} L_D Pr^{0.3} .$$

It possible to obtain a general equation for all the test specimens. The general equation is $Nu = 0.25 Re + 34.5$. **Figure 13** shows the relation between *Re* and *Nu* for general equation in the present work.

4. Conclusion

A method to fabricate cohesive diamond, graphite or short carbon fiber uniform dispersed copper matrix composites by powder mixing as well as powder coating followed by cold compaction and sintering was developed in this article. The influence of type of reinforcement and their surface treatment is investigated. The coated and uncoated diamond, graphite particles or short carbon fibers were well embedded and uniformly dispersed in the obtained copper matrix composites. The experimental results show that the increase in the electrical resistivity and decrease in the thermal conductivity of
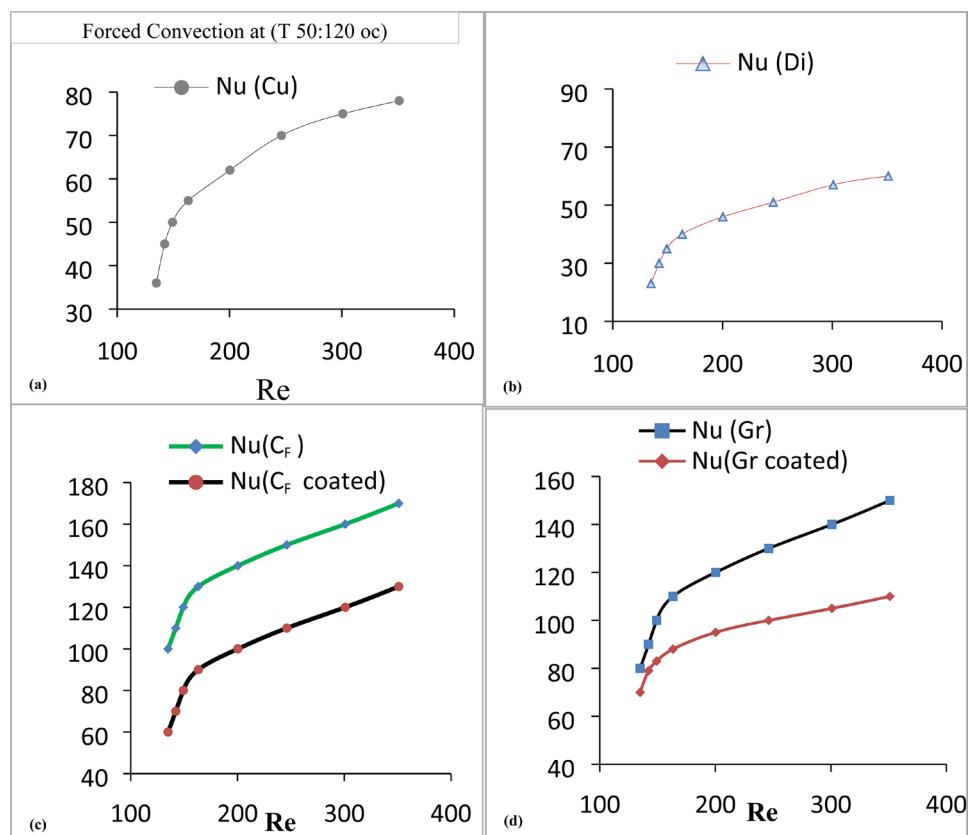
Figure 12. The relation between the (*Re*) and Nusselt number in cases of the forced convection.
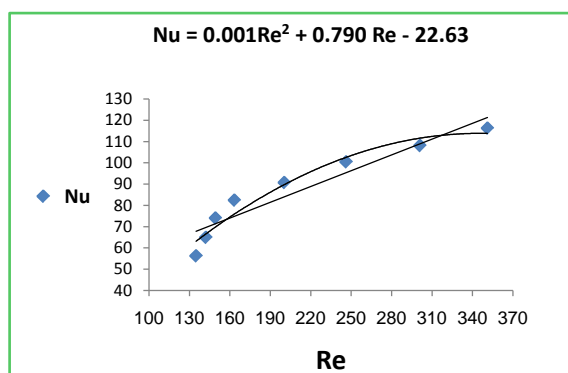

Figure 13. (*Re*) versus (*Nu*) number for the prepared specimens.

copper are due to the incorporation of the reinforcement particles as well as fibers in the copper matrix. However, the coating process of the reinforcements leads to the increase in effective thermal conductivity of composites and decreasing in the electrical resistivity. The signification increasing in the density, electrical and thermal conductivity of the copper based composites prepared from the coated particles could be due to the good interfacial bonding between the reinforcement particles and the *Cu* matrix. Due to the higher densification of the coated graphite particles and the coated short carbon fibers, the composites have showed higher electrical and thermal conductivities

as compared to those having uncoated particles and short fibers. Compared to the composites with uncoated particles or fibers, the particle intermediate coating greatly improved the interface bonding and decreased the interfacial electrical and thermal resistance of the copper base composites. These results indicated that the particle coating played a crucial role in the electrical and thermal properties of the copper base composites. This enhancement can be explained by the increase of electrical and thermal conductivity of the samples as due to the formation of conductive network by through the particles or short fibers. The new pretreatment coating method not only solves the interface problem with a lower price by a simple sintering furnace but also ensures the electrical and thermal conductivity of the copper matrix. The tested specimens were tested thermally by calculating natural and forced heat transfer. A general equation of heat transfer was conducted.

Acknowledgements

References

[1] Phase Ruch, P.W., Beffort, O., Kleiner, S., Weber, L. and Uggowitzer, P.J. (2006) Selective Interfacial Bonding in Al (Si)-Diamond Composites and Its Effect on Thermal Conductivity. *Composites Science and Technology*, **66**, 2677-2685. http://dx.doi.org/10.1016/j.compscitech.2006.03.016

[2] Chandra Sekhar Reddy, M. (2015) Thermal Analysis of a Heat Sink for Electronics Cooling. *International Journal of Mechanical Engineering and Technology* (*IJMET*), **6**, 145-153.

[3] Clyne, T.W. (2003) Thermal and Electrical Conduction in MMCs. In: Kelly, A., Chou, T.W., Talreja, R., Clyne, T.W., Warren, R., Carlsson, L., *et al.*, Eds., *Comprehensive Composite Materials*, *Metal-Matrix Composites*, Elsevier, Amsterdam, 3.

[4] Prieto, R., Molina, J.M., Narciso, J. and Louis, E. (2008) Fabrication and Properties of Graphiteflakes/Metalcomposites Forthermal Management Applications. *Scriptamateria*, **59**, 11-14.

[5] Chen, J.K. and Huang, I.S. (2013) Thermal Properties of Aluminium-Graphite Composites by Powder Metallurgy. *Composites Part B: Engineering*, **44**, 698-703. http://dx.doi.org/10.1016/j.compositesb.2012.01.083

[6] Abdel Hamid, Z., Moustafa, S.F., Morsy, F.A., Abdel AttyKhalifa, N. and Abdel Mouez, F. (2011) Fabrication and Characterization Copper/Diamond Composites for Heat Sink Application Using Powder Metallurgy. *Natural Science*, **3**, 936-947. http://dx.doi.org/10.4236/ns.2011.311120

[7] Weber, L. and Tavangar, R. (2007) On the Influence of Active Element Content on the Thermal Conductivity and Thermal Expansion of Cu-X (X = Cr, B) Diamond Composites. *Journal of Materials Science*, **57**, 988-991. http://dx.doi.org/10.1016/j.scriptamat.2007.08.007

[8] Schubert, T., Ciupinski, L., Zielinski, W., Michalski, A., Weigärber, T. and Kieback, B. (2008) Interfacial Characterization of Cu/Diamond Composites Prepared by Powder Metallurgy for Heat Sink Application. *Scripta Materialia*, **58**, 263-266. http://dx.doi.org/10.1016/j.scriptamat.2007.10.011

[9]   Daoush, W.M. and Elkady, O.A. (2014) Microstructure, Physical Properties and Hardness of Alumina Short Fibres/Nickel Matrix Composites Fabricated by Powder Technology. *Journal of Composite Materials*, **48**, 3735-3746. http://dx.doi.org/10.1177/0021998313513203

[10] Daoush, W.M. (2008) Processing and Characterization of CNT/Cu Nanocomposites by Powder Technology. *Journal of Powder Metallurgy and Metal Ceramics*, **47**, 531-537. http://dx.doi.org/10.1007/s11106-008-9055-x

[11] Daoush, W.M. and Moustafa, S.F. (2008) Coated Powders "a Good Base" for Intermetallics. *Metal Powder Report*, **62**, 16-18. http://dx.doi.org/10.1016/S0026-0657(09)70057-8

[12] Daoush, W.M. and Moustafa, S.F. (2007) Coating Points a Way for Synthesis of Tough Intermetallics. *Metal Powder Report*, **62**, 30, 32-33. http://dx.doi.org/10.1016/S0026-0657(07)70023-1

[13] Daoush, W.M., Lim, B.K., Mo, C.B., Nam, D.H. and Hong, S.H. (2009) Electrical and Mechanical Properties of Carbon Nanotube Reinforced Copper Nanocomposites Fabricated by Electroless Deposition Process. *Materials Science and Engineering*, **513-514**, 247-253. http://dx.doi.org/10.1016/j.msea.2009.01.073

[14] Deborah, C.D.L. (2001) Applied Materials Science Application of Engineering Materials in Structural. Electronics, Thermal and Other Industries, Chapman and Hall, London.

[15] Edelstein, A.S. and Cammarata, R.C. (1996) Nanomaterials: Synthesis, Properties and Applications. Taylor and Francis Group, London, 58.

[16] Schubert, T., Trindade, B., Weißgärber, T. and Kieback, B. (2008) Interfacial Design of Cu-Based Composites Prepared by Powder Metallurgy for Heat Sink Applications. *Materials Science and Engineering*, **475**, 39-44. http://dx.doi.org/10.1016/j.msea.2006.12.146

[17] Çengel, Y.A. and Ghajar, A.J. (2015) Heat and Mass Transfer Fundamentals & Applications. 5th Edition, Grawhil Education, Stillwater.

[18] Çengel, Y.A. and Zing, P.T.L. (1987) Enhancement of Natural Shrouding. *Proceedings of ASME/JSME Thermal Engineering Joint Conference*, Honolulu, 22-27 March 1987, 451-475.

[19] Churchill, S.W. (1977) A Comprehensive Correlating Equation for Laminar Assisting Forced and Free Convection. *AIChE Journal*, **23**, 10-16. http://dx.doi.org/10.1002/aic.690230103

[20] Churchill, S.W. (1983) Free Convection around Immersed Bodies. In: Schlünder, E.U., Ed., *Heat Exchanger Design Handbook*, Section 2,5,7, Hemispheres Publishing, New York, 500.

[21] Churchill, S.W. (1986) Combined Free and Forced Convection around Immersed Bodies. In: Schlünder, E.U., Ed., *Heat Exchanger Design Handbook*, Section 2,5,9, Hemispheres Publishing, New York, 230.

[22] Churchill, S.W. and Chu, H.H.S. (1975) Correlating Equations for Laminar and Turbulent Free Convection from a Horizontal Cylinder. *International Journal of Heat and Mass Transfer*, **18**, 1049-1053. http://dx.doi.org/10.1016/0017-9310(75)90222-7

[23] Churchill, S.W. and Chu, H.H.S. (1975) Correlating Equations for Laminar and Turbulent Free Convection from a Vertical Plate. *International Journal of Heat and Mass Transfer*, **18**, 1323-1329. http://dx.doi.org/10.1016/0017-9310(75)90243-4

[24] Eckert, E.R.G. and Soehngen, E. (1948) Studies on Heat Transfer in Laminar Free Convection with Zehnder-Mach Interferometer. USAF Technical Report, 5747.

[25] Eckert, E.R.G. and Soehngen, S.E. (1951) Interferometric Studies on the Stability and Transition to Turbulence of a Free Convection Boundary Layer. *Proceedings of the General Discussion on Heat Transfer*, London, 11-13 September 1951, 321-323.

[26] El Sherbiny, S.M., Raithby, G.D. and Hollands, K.G.T. (1928) Heat Transfer by Natural Convection across Vertical and Inclined Air Layers. *Journal of Heat Transfer*, **104**, 96-102. http://dx.doi.org/10.1115/1.3245075

[27] Fujiii, T. and Imura, H. (1972) Natural Convection Heat Transfer from a Plate with Arbitrary Inclination. *International Journal of Heat and Mass Transfer*, **15**, 755-767. http://dx.doi.org/10.1016/0017-9310(72)90118-4

[28] Hollands, K.G.T., Unny, T.E., Raithby, G.D. and Konicek, L. (1976) Free Convective Heat Transfer across Inclined Air Layers. *Journal of Heat Transfer*, **98**, 189-193. http://dx.doi.org/10.1115/1.3450517

[29] Holman, J.P. (1990) Heat Transfer. 7th Edition, McGraw Hill, New York.

[30] Incropera, F.P. and DeWitt, D.P. (1996) Introduction to Heat Transfer. 3rd Edition, John-Wile & Sons, New York.

[31] Jakob, M. (1949) Heat Transfer. Wiley, New York.

[32] Kays, W.M. and Crawford, M.E. (1993) Convective Heat and Mass Transfer. 3rd Edition, McGraw Hill, New York.

[33] Kreith, F. and Bohn, M.S. (2001) Principles of Heat Transfer. 6th Edition, Brooks/Cole, Pacific Grove.

[34] Cullity, B.D. (1956) Elements of X-Ray Diffraction. Addison-Wesley, Upper Saddle River, 1-110.

[35] Chu, K., Jia, C.C., Guo, H. and Li, W.S. (2013) On the Thermal Conductivity of Cu–Zr /Diamond Composites. *Materials and Design*, **45**, 36-42. http://dx.doi.org/10.1016/j.matdes.2012.09.006

[36] He, J.S., Zhang, H.L., Zhang, Y., Zhao, Y.M. and Wang, X.T. (2014) Effect of Boron Addition on Interface Microstructure and Thermal Conductivity of Cu/Diamond Composites Produced by High Temperature-High Pressure Method. *Physica Status Solidi* (*A*), **211**, 587-594. http://dx.doi.org/10.1002/pssa.201330237

[37] Mankowski, P., Dominiak, A., Domanski, R., Kruszewski, M.J. and Ciupinski, L. (2014) Thermal Conductivity Enhancement of Copper-Diamond Composites by Sintering with Chromium Additive. *Journal of Thermal Analysis and Calorimetry*, **116**, 881-885. http://dx.doi.org/10.1007/s10973-013-3604-3

[38] Li, J.W., Wang, X.T., Qiao, Y., Zhang, Y., He, Z.B. and Zhang, H.L. (2015) High Thermal Conductivity through Layer Optimization in Diamond Particles Dispersed Zr-Alloyed Cu Matrix Composites. *Scripta Materialia*, **109**, 72-75. http://dx.doi.org/10.1016/j.scriptamat.2015.07.022

[39] Davis, J.R. (2001) ASM Specialty Handbook (Copper and Copper Alloys). ASM International, USA.

[40] Kim, C., Lim, B., Kim, B., Shim, U., Oh, S., Sung, B., Choi, J., Ki, J. and Baik, S. (2009) Strengthening of Copper Matrix Composites by Nickel-Coated Single-Walled Carbon Nanotubes Reinforcements. *Synthetic Metals*, **159**, 424-429. http://dx.doi.org/10.1016/j.synthmet.2008.10.017

[41] Chu, K., Guo, H., Jia, C., Yin, F., Zhang, X., Liang, X. and Chen, H. (2010) Thermal Properties of Carbon Nanotube-Copper Composites for Thermal Management Applications. *Nanoscale Research Letters*, **5**, 868-874. http://dx.doi.org/10.1007/s11671-010-9577-2

[42] Eucken, A. (1932) Thermal Conductivity of Ceramic Refractory Materials, Calculation from Thermal Conductivity of Constituents. *Ceramic Abstracts,* **11**, 353-360.

Scientific Research Publishing

Submit or recommend next manuscript to SCIRP and we will provide best service for you:

Accepting pre-submission inquiries through Email, Facebook, LinkedIn, Twitter, etc.

A wide selection of journals (inclusive of 9 subjects, more than 200 journals)

Providing 24-hour high-quality service

User-friendly online submission system

Fair and swift peer-review system

Efficient typesetting and proofreading procedure

Display of the result of downloads and visits, as well as the number of cited articles

Maximum dissemination of your research work

Submit your manuscript at: http://papersubmission.scirp.org/

Or contact msa@scirp.org